Computer Simulation Study of the Structure of LiCl Aqueous Solutions: Test of Non-Standard Mixing Rules in the Ion Interaction

Juan L. Aragones,[†,‡] Mauro Rovere,[†] Carlos Vega,[‡] and Paola Gallo*[,†,§]

[†]Dipartimento di Matematica e Fisica, Università Roma Tre, Via della Vasca Navale 84, 00146 Roma, Italy
[‡]Departamento de Química Física, Facultad de Ciencias Químicas, Universidad Complutense de Madrid, 28040 Madrid, Spain
[§]INFN Roma Tre, Via della Vasca Navale 84, 00146 Roma, Italy

Ⓢ *Supporting Information*

ABSTRACT: Aqueous solutions of LiCl have recently received much attention in connection with the study of the anomalies of supercooled water and its polymorphism. From the point of view of computer simulation, there is need for a force field that can reproduce the structural and dynamical properties of this solution, and more importantly it is also simple enough to use in large scale simulations of supercooled states. We study by molecular dynamics the structure of the LiCl–water solutions with the force field proposed by Joung and Cheatham (*J. Phys. Chem. B* **2008**, *112*, 9020) appropriate for the water TIP4P-Ew model potential. We found that this force field does not reproduce the experimental ion pairing when the Lorentz–Berthelot (LB) rules are used. By incorporating deviations to the LB rules to obtain the crossed interactions between the ions, it is possible to get agreement with experiment. We have studied how the modification of the LB rule affects the structural and thermodynamic properties of the solution at increasing concentration of the solution from the low (around 2%) to medium (around 14%) concentration regimes. We also tested the transferability of the Joung and Cheatham force field to the water TIP4P/2005 model that works very well for supercooled water.
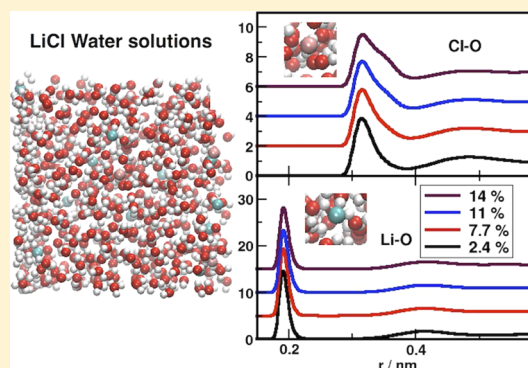
1. INTRODUCTION

Aqueous solutions of salts are systems of great importance in many fields connected to chemistry, biochemistry, chemical engineering, etc. In this respect, solutions of simple salts represent prototypes for the study of more complex systems.[1,2] In particular, aqueous solutions of LiCl, the salt with the smallest cation, have frequently been considered for thermodynamic and structural studies due to their very good solvation properties; LiCl presents in fact a high solubility.[3] The solubility of LiCl(solid) in water at room temperature extrapolated from high temperature measurements is about $25m$[4] (i.e., moles of LiCl per kilogram of water), although the solubility of the hydrated solid $LiCl \cdot H_2O$ at room temperature is somewhat lower, $20m$,[4,5] so that it precipitates first from solution. Diffraction experiments of X-rays or neutrons have been extensively carried out on this system[6−12] and coupled with reverse Monte Carlo techniques.[13−15] Computer simulation studies have been performed with different model potentials.[13,16−20]

Renewed interest in LiCl aqueous solutions (LiCl(aq)) has grown due to experiments addressed to understand the polymorphism of water.[12,21−23] Key questions in the study of supercooled ionic solutions are from one side how the relevant changes in the behavior of water upon cooling could affect its properties as a solvent,[24−26] and on the other side how the anomalies of water can be modified by solvated ions.[27−30]

Therefore, the topic concerned with the structural and dynamical properties in the deeply supercooled liquid state of LiCl(aq) is the theme of a present vivid debate.

With the idea of future applications of computer simulation to the study of LiCl(aq) upon supercooling, or in its glassy phases, it is a relevant matter to test simple two body potentials that can be used in large computational calculations. Given the relevance of these systems, many computational works have been devoted to the development of a good force field that could reproduce the main features of the water salt solutions, and different approaches have been applied. Several groups have studied salt solutions by means of *ab initio* molecular dynamics (MD) simulations.[31−34] However, the high computational cost of this approach restricts its application to problems of short time and small size scales. In addition, it has been shown that the polarization of the first hydration shell due to the ions is negligible (except for orientational contributions).[33] The effects of the ions extend only to the first hydration shell, and they are independent of the size or charge of the ions.

Therefore, the explicit account of the polarizability on these studies may be not strictly necessary.

The use of empirical, standard pairwise additive and nonpolarizable intermolecular potentials presents some advantages with respect to the *ab initio* methods, such as its reduced computational cost, and the transferability to more complex systems such as biological matter, for which the majority of codes and force fields use this approach. Other attempts including polarization effects have also been tried.[35,36] However, the computational cost is significantly increased, and for the majority of biological codes and force fields, these contributions are neglected.

Several attempts to parametrize ions in water have been carried out.[37,38] The ionic force fields are usually based on the combination with an already tested model for pure water. Jensen and Jorgensen[39] developed a force field around the TIP4P water potential model.[40] They focused on the hydration free energy and first maximum of the ion−water radial distribution function (RDF). Smith and Dang[41,42] parametrized the Na^+ and Cl^- ions based on a three-site polarizable water model[43] and the SPC/E model,[44] fitting to both experimental quantities, gas-phase binding enthalpies for small ion−water clusters and the structure and solvation enthalpies of ionic solutions. More recently, Joung and Cheatham[45] have carried out an extensive study in order to parametrize alkali metal cations and halide anions (JC parameters). One of the primary motivations of the development of the JC parameters was the spontaneous aggregation of certain salts on DNA in molecular simulations.[46] This force field was tailored for three different well-known water potential models, TIP3P,[40] SPC/E, and TIP4P-Ew.[47] They used a more complex space of properties to adjust the parameters of the Lennard-Jones (LJ) ionic potential. As in the rest of the previous works, they targeted the free energy of hydration for individual ions, the gas phase ion−water interaction energies, and the ion−water radial distribution function (RDF). However, they have also included properties of the alkali halide solid phases, such as the lattice energies and lattice constants, in order to avoid the spontaneous aggregation of ions around DNA by balancing the crystal and solution phases. In all of these approaches, only properties that do not directly match ion−ion interactions in solution have been used as target properties. In the calculations of structural properties of aqueous solutions of salts, it is usual to focus mainly on the distributions of ions around water and the modification induced by ions on the structure of water, while less attention is paid to the ion−ion correlation probably due to the absence of experimental feedback. Therefore, the majority of these force fields fails to reproduce the ion pairing.

Another recent attempt to optimize ionic force fields has been carried out by Fyta et al. Focusing on this missing information on previous ionic force fields, they based their force field optimization on single-ion and ion-pair solvation properties.[48] Interestingly, they showed that within the LJ-dimensional space and Lorentz−Berthelot (LB) combining rules, it is not possible to parametrize anions to simultaneously reproduce single ion properties and ion pairing properties.[48] Thus, the conclusion seems to be that force fields constructed as LJ-like and based on the standard LB mixing rules are not able to reproduce simultaneously the single-ion and ion pairing properties. The next step in the optimization of ionic force fields is based on the modification of the mixing rules to obtain the ion−ion crossed interactions,[20,32,35,49,50] which in addition may allow *water-free* ionic force fields to be built[51] or it may

allow to parametrize ions independently on their ion pair.[52] In other words, by fitting the crossed interactions between water−ions and ion−ion, it would be possible to build a transferable ionic force field.

The pairwise additive ionic force fields moreover are tailored for a particular water potential. The water model must be chosen according to its performance in reproducing the properties of pure water, although no model reproduces all water properties.[53,54] Since the choice of the ion model is usually biased for the water model, it is relevant to check the transferability of the ion potential to other water models.[17,55]

In this paper, we consider, in order to determine the structure of aqueous solutions of LiCl, the force fields recently proposed by Joung and Cheatham (JC)[45] around the TIP4P-Ew, which represents some improvements with respect to other options. In addition, and given that the TIP4P-Ew parametrization *philosophy* is similar to the TIP4P/2005 (i.e., geometry, target properties, application of the Berendsen polarization correction[44]), we have tested the transferability of the LiCl JC force field to the TIP4P/2005.[56] The possibility of using the TIP4P/2005 together with the JC ion potential presents some advantages for the purpose of future works under supercooled conditions, where this potential has been successfully tested.[57] In order to improve the prediction of the ion pairing, we check the force field to be used in our case by considering the ion−ion structure. We compare the results of our simulation with the experimentally estimated ion pairing recently obtained with the neutron scattering technique.[12] We introduce a modification of the ion−ion mixed interaction to improve the agreement with the experimental estimates. We compare the results obtained with the normal and modified mixing rules.

In the next section, we give the details of our computer simulation. In section 3, we show how to modify the force field in order to reproduce an ion contact in agreement with the experiments. The ion structures then are studied at different concentrations. In section 4 and 5, we present the results respectively for the water structure and the ion hydration at increasing ionic concentrations. In section 6, tables with thermodynamic results and the behavior of the diffusion coefficients are presented. In section 7, we present our test of transferability of the JC force field. Finally, section 8 is devoted to the conclusions.

2. SIMULATION DETAILS AND MOLECULAR MODELS

In order to study the structure of the LiCl water solutions, we consider the JC force fields.[45] We have adopted for our study the force field associated with the TIP4P-Ew. This water potential model in fact is able to reproduce a great number of liquid water properties. The TIP4P-Ew potential, a modification of the previous TIP4P model,[58] is a rigid four-site model, where hydrogens (H) are represented by two positively charged sites connected to a neutral oxygen (O) site. The negative charge of O is on a site (M) shifted by 0.0125 nm in the molecular plane. The oxygen sites of the water molecules interact with a Lennard-Jones potential. Therefore, the potential of the ionic solution is written as a combination of a LJ and a Coulombic potential

$$U(r_{ij}) = 4\varepsilon_{ij}\left[\left(\frac{\sigma_{ij}}{r_{ij}}\right)^{12} - \left(\frac{\sigma_{ij}}{r_{ij}}\right)^{6}\right] + \frac{q_i q_j}{4\pi\varepsilon_o r_{ij}}$$

(1)

where r_{ij} is the distance between two interacting particles and q_i is either the charge of an ion or the charge of a water site. The JC parameters for LiCl(aq) are presented in Table 1, as well as the parameters of the TIP4P-Ew potential.

Table 1. Parameters for the Joung−Cheatham Force Fields and TIP4P-Ew and TIP4P/2005 Water Models[a]

LJ interaction	ε/k_B (K)	σ (nm)	charge		q (e)	d_{OM} (Å)
		Water TIP4P-Ew				
O−O	81.9	0.316 43	O		0.0	0.125
			M		−1.0484	
			H		0.5242	
		Water TIP4P/2005				
O−O	93.2	0.315 89	O		0.0	0.1546
			M		−1.1128	
			H		0.5564	
		Joung−Cheatham				
Li$^+$−Li$^+$	52.3293	0.143 97			+1.0	
Cl$^-$−Cl$^-$	5.8683	0.491 78			−1.0	

[a]The crossed interactions can be obtained through eq 2. The angle formed by hydrogen, oxygen, and the other hydrogen atom is 104.52°, and the oxygen−hydrogen distance is 0.09552 nm for both water models TIP4P-Ew and TIP4P/2005. d_{OM} is the distance of the negative charge on the H−O−H bisector. The LJ site is located at the oxygen. σ and ε/k_B are the LJ parameters and q the charge.

The crossed interactions can be written as

$$\varepsilon_{ij} = \chi \cdot \sqrt{(\varepsilon_{ii} \cdot \varepsilon_{jj})}; \qquad \sigma_{ij} = \eta \cdot \frac{\sigma_{ii} + \sigma_{jj}}{2} \tag{2}$$

where i,j represents the species involved. In the original JC potential, as in the TIP4P-Ew, the LB combining rules are assumed and the parameters χ and η take the unit value. The LB rules can be modified by changing χ and η. As discussed in section 3, we modified these parameters only for the ion−ion interaction in order to get a better agreement with experiment for the ion−ion contact.

For the rest of the paper, we consider results obtained with the use of the LB mixing parameters to be compared with results obtained with modified LB (MLB) rules for the ion interactions. LB rules are always used to describe water−ion interactions. Thus, the notation LB/MLB refers to whether LB rules were used or not to describe ion−ion interactions. We expect the main effects of the MLB rules on the RDF of the ions, but we will check how relevant are the changes in the hydration properties and the water−water structure at increasing concentrations.

The simulations were performed at increasing percentage moles of solute, indicated as $100 \times n_s/(n_s + n_w)$. The correspondent concentrations in mol/kg are given in Table 2.

Let us now provide some details about simulation runs. Molecular dynamic simulations were performed using Gromacs[59] (version 4.5). We used a velocity scaling thermostat[60] to keep T fixed at 298 K and a Parrinello−Rahman barostat[61] to keep pressure constant at 0.1 MPa. The relaxation

time for the thermostat and barostat was 2 ps. The LJ interaction was smoothly switched off between 0.90 and 0.95 nm, and a standard long-range correction was employed. Ewald sums were used to deal with the Coulombic interactions. The real part of the Coulombic interaction was truncated at 0.95 nm, and the reciprocal contribution was evaluated by using PME.[62] We performed the simulations on 480 water molecules. The number of anions (cations) is, for growing concentrations, 12, 15, 20, 22, 30, 40, 60, and 80. Long simulations were performed in order to obtain accurate results, even when the number of ions is small (i.e., 2.4%). The typical simulation length was 70 ns, and the time step was 2 fs. We equilibrated the initial configurations by about 2 ns. Constraints were used to fix the geometry of the molecule of water by using the SETTLE algorithm.[63] The results were obtained by running Gromacs in parallel using 4 CPUs; with this number of processors, we typically obtained 45 ns/day.

In order to compare the results with the experiments,. we have also computed the neutron interference differential cross sections $(F^N(Q))$ of LiCl aqueous solutions. The scattered radiation amplitude from N nucleus at positions $r_1, ..., r_N$ is given by

$$S(Q) = \sum_{j=1}^{N} b_j e^{(i\mathbf{Q} \cdot \mathbf{r}_j)} \tag{3}$$

where b_j is the scattering amplitude of the atom j,[64] which is independent of $\mathbf{Q}$ and characteristic of the isotope and spin states of the nucleus. $\mathbf{Q}$ is the wave-vector, $\mathbf{Q} = |Q| = 4\pi(\sin\theta/\lambda)$, and $\mathbf{r}_j$ is the position of the nucleus j. Then, the scattered intensity per atom is given by

$$I(\lambda, 2\theta) = \frac{1}{N}|S(\mathbf{Q})|^2 \tag{4}$$

Neutron scattered intensity splits into *self* and *interference* terms.[65] Therefore, it is common to carry out a normalization of the data, usually by defining a neutron interference differential cross section:

$$F^N(Q) = I(\lambda, 2\theta) - \sum_{\alpha} c_{\alpha} \langle b_{\alpha}^2 \rangle \tag{5}$$

where c_{α} is the atomic fraction of the component α. Notice that $\langle b_{\alpha}^2 \rangle$ may be different from $\langle b_{\alpha} \rangle^2$.[65]

## 3. POTENTIAL MODEL AGAINST EXPERIMENT: ION CONTACT

In order to check the force field to be used in our case, we consider the ion−ion structure by comparing the results of simulation with the experimentally estimated ion pairing recently obtained with the neutron scattering technique for the concentration of 2.4%.[12] From now on, we will refer to it as experimental RDFs.

In Figure 1, we show the LiCl RDF calculated with the LB rules ($\chi = 1.0$ and $\eta = 1.0$) and compared with the experimental one.[12] For the standard combination rules, the $g_{LiCl}(r)$ correctly

Table 2. Concentrations Adopted in Our Simulations[a]

%	2.4	3.0	4.0	4.4	5.9	7.7	11.0	14.0
mol/kg	1.38	1.74	2.30	2.54	3.47	4.63	6.94	9.25
N_{LiCl}	12	15	20	22	30	40	60	80

[a]The number of water molecules is 480 in all cases.
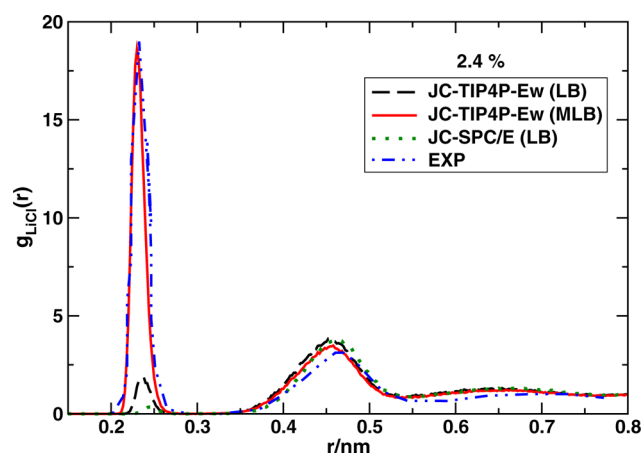
Figure 1. Li−Cl RDF for molar percentage 2.4% at 298 K and 0.1 MPa. Long dashed line: result of the JC-TIP4P-Ew parameters using LB rules. Bold line: result of the JC-TIP4P-Ew parameters using MLB rules. Point line: result of the JC-SPC/E parameters with LB rules. Point dashed line: experimental result.[12]

shows a first maximum at $r = 0.236$ nm and a second peak at around $r = 0.475$ nm, indicating that Li and Cl ions are approximately separated by one molecule of water, as found in experiment. However, the first maximum is underestimated and it is less intense than the second peak in clear disagreement with the experimental results. The same trend is observed for the JC-SPC/E parameters, but the discrepancy is indeed greater. We optimized the mixing interaction by varying the parameters χ and η in eq 2. The new values $\chi = 1.88$ and $\eta = 0.932$ give the result in Figure 1. The intensity of the first peak is correctly recovered. In the following, we will use these parameters for the calculations with the MLB rules.

However, ion−ion partial radial distribution functions cannot be determined unambiguously from neutron scattering measurements. Therefore, to further test the performance of the JC-TIP4P-Ew force field reproducing the LiCl solution structure, we have also computed the neutron interference differential cross section from our MD simulations for the
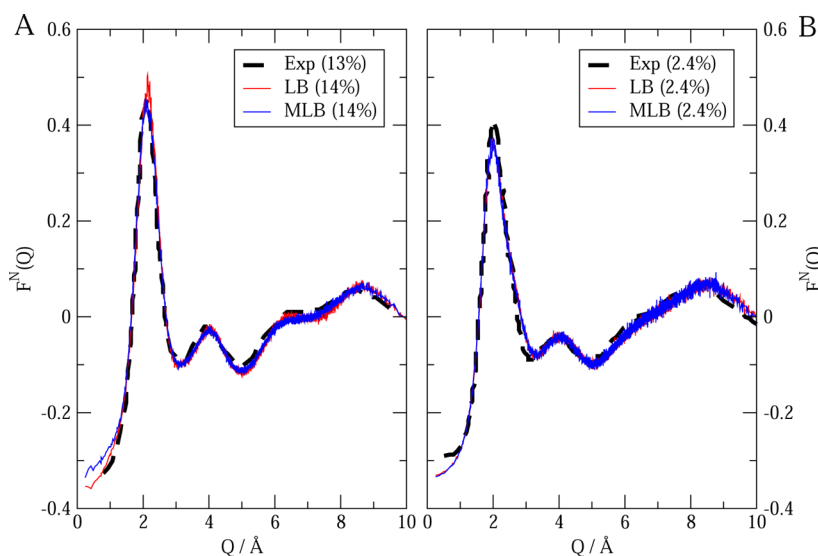
highest and lowest concentrated LiCl solutions considered in this work, and compared them with the experimental ones (Figure 2). As it can be seen in Figure 2A, the agreement for the most concentrated solution considered in this work is quite satisfactory. The main difference is the height of the first maximum, higher for the $F^N(Q)$ obtained from MD simulations. However, when modifications to the LB rules are considered, the height of the first maximum is also reproduced. For the lowest concentration, Figure 2B, the effect of including modification to the standard combination rules does not show changes in the differential cross sections, because O−D and D−D correlations dominate.[14,15] Good agreement is then achieved using both LB and MLB rules.

The $g_{LiCl}(r)$ values at increasing concentration are shown in Figure 3, both using LB and MLB rules. With the LB rules, the
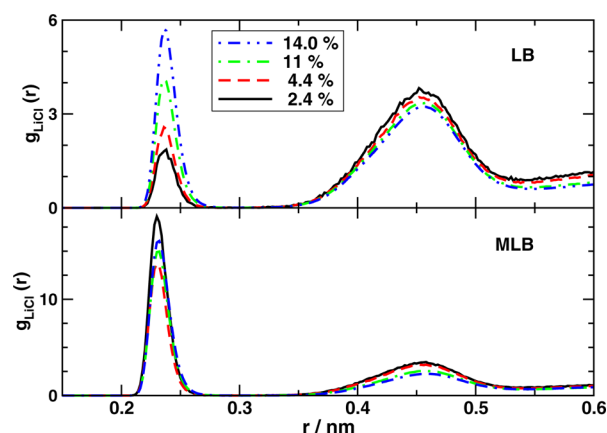
Figure 3. Li−Cl RDF as a function of salt concentration, using LB rules (top) and MLB rules (bottom) at 298 K and 0.1 MPa. The results are shown only for four concentrations in order to show more clearly the trend.

intensity of the first peak increases monotonically with the concentration. On the contrary, with the application of the MLB rules, the highest first peak is obtained at the lowest

Figure 2. Differential cross sections of LiCl aqueous solutions for two different concentrations, the highest concentration 14.0% (A) and the lowest concentration 2.4% (B), and compared with the experimental ones 13%, replotted from Figure 3 of ref 15 and 2.4%, replotted from Figure 1 of ref 12 (black lines). Using LB rules (red lines) and using MLB rules (blue lines).

concentration, and its intensity is reduced when the concentration is increased, in agreement with experiments. Other trends obtained with MLB in agreement with experiments are the little increase with concentration of the distance between the first and second peaks[12] and the increase of the anion−cation contacts. The anion−cation contact pairs can be easily obtained from $g_{LiCl}(r)$:

$$n_{Li}^{Cl} = 4\pi\rho_{Li^+} \int_0^{r_1} g_{LiCl}(r)r^2\,dr \tag{6}$$

where ρ_{Li^+} is the Li^+ number density and r_1 the position of the first minimum. The results are tabulated in Table 3. We observe

Table 3. Anion−Cation Contact Pairs (n_{Li}^{Cl}) at the Lowest and Highest Concentrations Considered in This Study Using Both LB and MLB Rules

%	LB	MLB
2.4	0.02	0.19
14.0	0.39	1.01

that the number of LiCl ion pairs (n_{Li}^{Cl}) at the lowest concentration is very small, close to zero, if we use LB combining rules. It is instead about 0.2 using MLB rules, in agreement with the experiment.

The Li−Li and Cl−Cl RDFs are reported in Figures 4 and 5. The $g_{LiLi}(r)$ presents, similar to experiment, a broad peak at
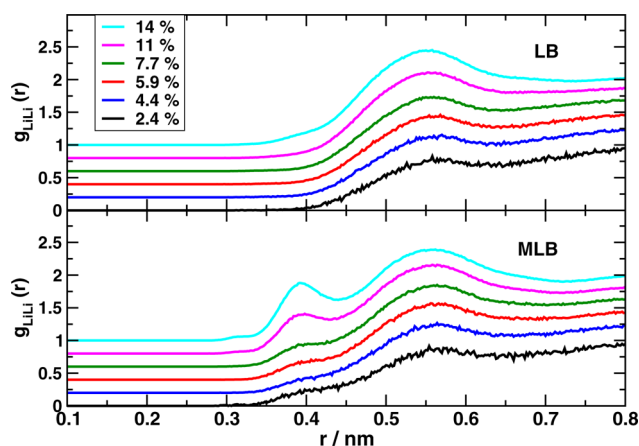
Figure 4. Li−Li RDF as a function of salt concentration, using LB rules (top) and MLB rules (bottom). Every curve is shifted by 0.2 in vertical from the previous one.

∼0.55 nm. The intensity of this maximum increases with the concentration. However, applying MLB rules, we observe the appearance of a prepeak at lower distances (0.39 nm) when the concentration increases. This prepeak is located at the same position as the one observed in experiment on hyperquenched samples,[12] but also incipient at ambient temperature, it has been assigned to the water separated contacts. The increase of the prepeak with concentration could indicate a tendency to phase separation or *clusterization*, as predicted at higher pressures,[66] and observed in simulation with another force field.[26]

As shown in Figure 5, a prepeak appears in the $g_{ClCl}(r)$ at high concentrations with the LB rules, while with the MLB potential a small prepeak is present even at the lowest concentration and the effect of the increasing concentration is enhanced.
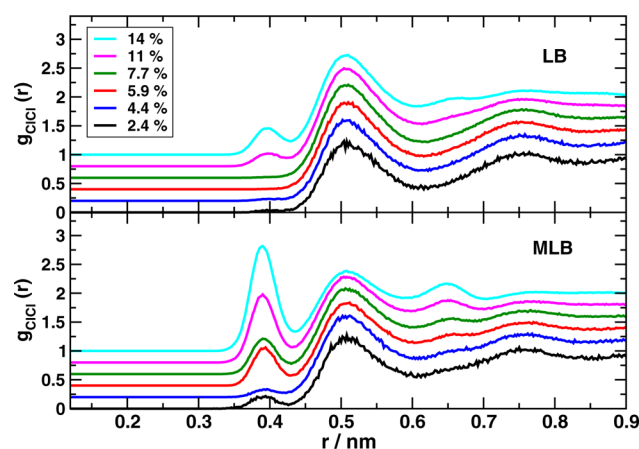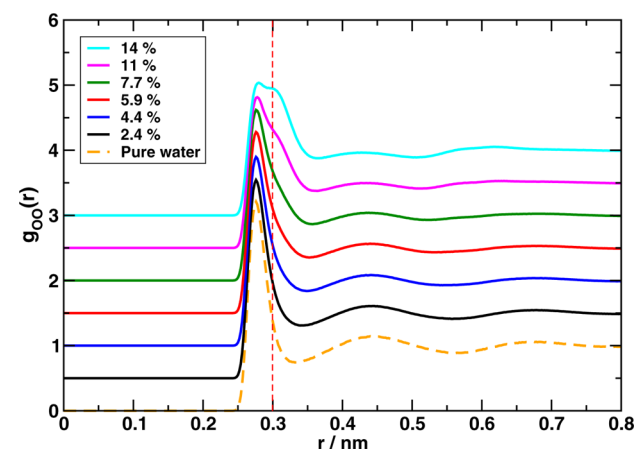

Figure 5. Cl−Cl RDF as a function of salt concentration, using LB rules (top) and MLB rules (bottom). Every curve is shifted by 0.2 in vertical from the previous one.

Summarizing, the number of LiCl pairs increases when using the MLB combining rules as compared to the results obtained with the LB rules. In addition, if using the MLB rules, the tendency of the system to form larger clusters also increases. Some snapshots showing the positions of the ions in the most diluted solution when using LB rules or MLB rules are provided as Supporting Information.

4. WATER STRUCTURE

In Figures 6 and 7, we report the RDF of the oxygen water sites at increasing concentration of the solute obtained with LB and

Figure 6. Oxygen−oxygen RDF in LiCl solutions as a function of salt concentration with the use of LB rules. Every curve is shifted by 0.5 in vertical from the previous one.

MLB rules, respectively. From the figures, it is evident that, in the case of LB potential, the increasing concentration of LiCl has a strong effect on the oxygen−oxygen RDF, which reflects the perturbation of the water tetrahedral network due to the ion−water interactions.

The second peak of the bulk $g_{OO}(r)$ at 0.45 nm in particular is depressed accompanied by a broadening of the first peak. The depressing of the second $g_{OO}(r)$ peak is related with the distortion of the tetrahedral network, since it is located at $\approx 0.28(8/3)^{1/2}$, the tetrahedral second-neighbor distance corresponding to a nearest-neighbor distance of 0.28 nm. For the concentration of $c = 5.9\%$, a shoulder appears on the right
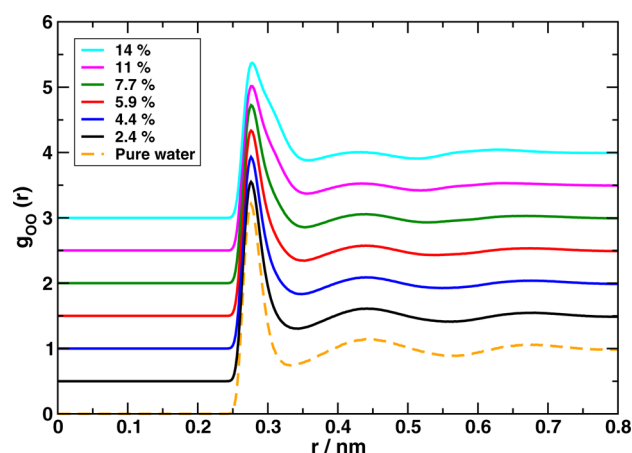
Figure 7. Oxygen–oxygen RDF in LiCl solutions as a function of salt concentration with the use of MLB rules. Every curve is shifted by 0.5 in vertical from the previous one.

side of the first peak. It evolves to form a second peak at 0.3 nm for $c = 14\%$. The appearance of a second peak at approximately the same position, 0.3 nm, in $g_{OO}(r)$ at increasing solute concentration is in agreement with previous results of computer simulations.[26] This is consistent with a densification of the water due to the presence of ions: water molecules densified at the ion hydration shells.

By considering MLB parameters, the same structural changes on the O–O are observed with differences at high concentrations, since a broadening on the high r side of the first peak appears, but it does not evolve in a secondary peak; see Figure 7. Trends found in KCl and NaCl aqueous solutions[67] are more similar to the MLB case.

As seen in Figure 8, the OH and HH RDFs are almost unchanged with respect to pure water for all of the concentrations. The hydrogen bond (HB) peak appears almost unaffected by the presence of ions apart for a broadening at high ion concentration, consistent with a HB distortion due to the solutes.

Therefore, the main effect of the inclusion of ion on the structure of water consists of a distortion of the HB network, evidenced by the strong changes in the second shell of the OO RDF, while the hydrogen bonds are preserved. This has been found in different ionic aqueous solutions,[28,67,68] and it implies that ions mimic the effect of an increase of pressure on water. Equivalent results are obtained with MLB.

5. HYDRATION SHELLS

When we consider the oxygen-ion RDFs, shown in Figures 9 and 10 for the LB and MLB rules, we note that the first shell of the Li$^+$ is very well-defined and close to the oxygens, while the corresponding first shell of Cl$^-$ is broader. For both cations and anions, the position of the first hydration peak does not change with ion concentration. It is located at around 0.195 nm for LiO and 0.315 for ClO, with the same values obtained in the experiment on the 2.4% solution.[12] By comparing with the Li–Cl RDF in Figure 3, we observe that the anion hydration shell can contain contact ion pairs, while this is highly unlikely within the Li$^+$ hydration shell. This is an interesting asymmetry in the hydration shells of ions in water.

The hydration shell of the Li$^+$ ions is slightly modified by the change in concentration (Figure 9). However, the opposite trend is observed with the application of the MLB rules. As the
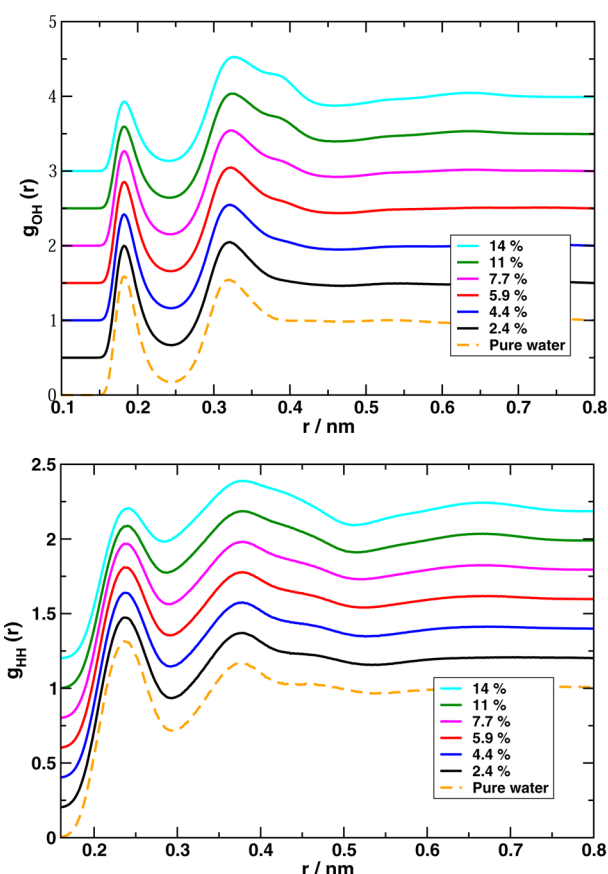

Figure 8. Oxygen–hydrogen (top) and hydrogen–hydrogen (bottom) RDF in LiCl solutions as a function of salt concentration with the use of LB rules at 298 K and 0.1 MPa. Every OH (HH) curve is shifted by 0.5 (0.2) in vertical from the previous one.
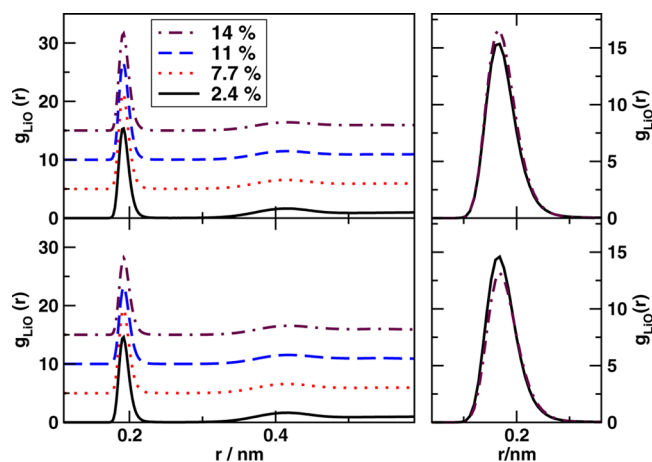
Figure 9. LiO RDF for four concentrations using LB rules (panels on the top) and MLB (panels on the bottom) at 298 K and 0.1 MPa. In the panels on the right are comparisons of the first peak on an enlarged scale in r for the lowest and highest concentrations. In the panels on the left, every curve is shifted by 5 in vertical from the previous one.

concentration increases, the first peak intensity increases with LB rules and decreases when MLB rules are applied. On the same direction, the Cl$^-$ hydration shell is hardly affected by the concentration increase, but it changes significantly due to the modification of the LB rules. With the LB rules, the ClO RDF
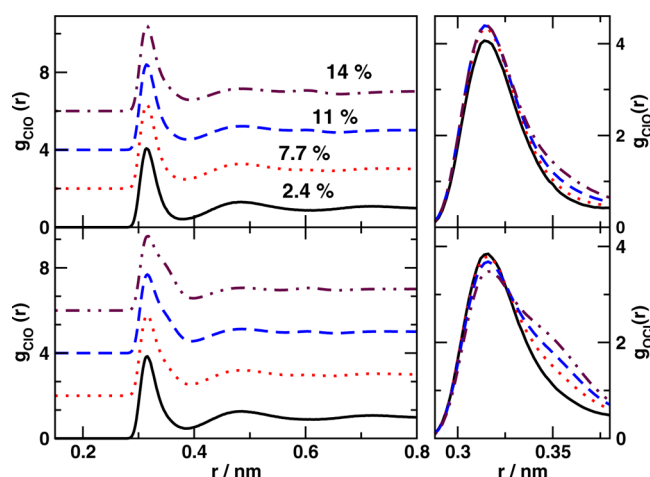
Figure 10. ClO RDF for four concentrations using LB rules (panels on the top) and MLB (panels on the bottom) at 298 K and 0.1 MPa. In the panels on the right are comparisons of the first peak on an enlarged scale in r for the four concentrations.

shows that the increase of the presence of salt has little effect on the Cl^- hydration shell with a small broadening of the peak and a consequent shift of the first minimum to higher distances. However, when the MLB rules are applied, the changes in the ion hydration shells are more marked (Figure 10). At increasing concentration, the first shell broadens with the appearance of a shoulder around 0.34 nm while the intensity of the second peak slightly decreases. The deviation from the LB rules appears to favor the hydration of the anion due to the broadening of the first shell, while an opposite effect is found for Li^+; see Figures 9 and 10.

The numbers of water molecules around the ions are reported for the lowest and highest concentrations in Table 4.

Table 4. Hydration Shells

concentration	ion	number of water molecules	
		LB	MLB
2.4%	Li^+	4.0	3.8
	Cl^-	6.6	7.1
14%	Li^+	3.5	3.2
	Cl^-	6.1	6.6

Both around cations and anions, the number decreases with concentration. By considering that the contact numbers of the LiCl increases with concentration, we can say that these results show a tendency of the ions to clusterization with increasing concentrations.

In Figure 11, we show on the same plot the $g_{OO}(r)$, g_{LiO}, and g_{ClO} calculated with MLB rules. With the oxygen site in the origin, there is evidence of a sort of charge ordering with a rigid shell of Li^+ cations close to the origin, while the shells of Cl^- anions and O are in the minimum of the Li−O RDF. There is a large penetration of Cl^- into the O shell and also of O into the Cl^- shell. These penetration effects are more marked for the highest concentration. It appears that Cl^- could be substitutive to oxygens. The behavior of the $g_{OO}(r)$ and $g_{ClO}(r)$ (Figure 11) is very similar, although the number of water molecules around oxygens is 4.2−4.3 while around anions the number is 6−7 (see Table 4), since Cl^- are about 50% larger.
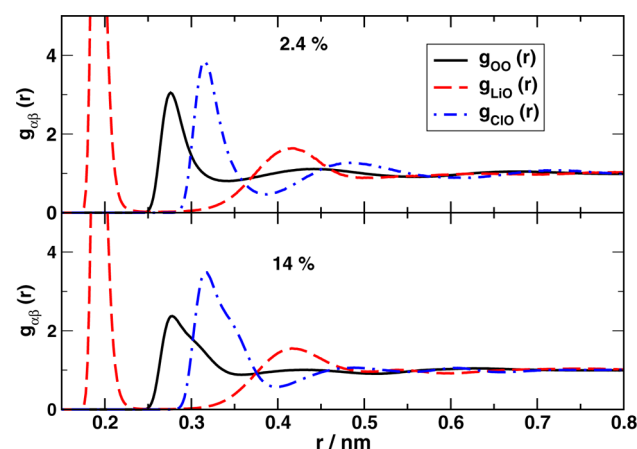
Figure 11. O−O, Cl−O, and Li−O RDFs for the lowest and highest concentrations at 298 K and 0.1 MPa (MLB rules).

6. THERMODYNAMIC AND KINETIC PROPERTIES

As shown in Tables 5 and 6, the internal energies, volumes, and densities of the solutions are almost unaffected by the

Table 5. Thermodynamic Results Using LB Rules[a]

N_{ions}	%	mol/kg	U (kJ/mol)	V (nm^3)	ρ (g/cm^3)	ϕ
24	2.4	1.38	−65.81	14.876	1.022	0.587
30	3.0	1.73	−70.36	14.992	1.028	0.595
40	4.0	2.30	−77.71	15.188	1.038	0.608
44	4.4	2.54	−80.57	15.266	1.042	0.614
60	5.9	3.47	−91.59	15.591	1.056	0.634
80	7.7	4.63	−104.47	16.003	1.073	0.657
120	11.0	6.94	−127.47	16.868	1.101	0.699
160	14.0	9.25	−147.43	17.747	1.126	0.736

[a]Internal energies are given in kJ mol^{-1} (per mol of particles $N_+ + N_-$ + N_{H_2O}). The number of water molecules is 480 for each solution. ϕ is the packing fraction of the solution ($\phi = (\pi/6)(1/V)\sum_I N_i \sigma_i^3$).
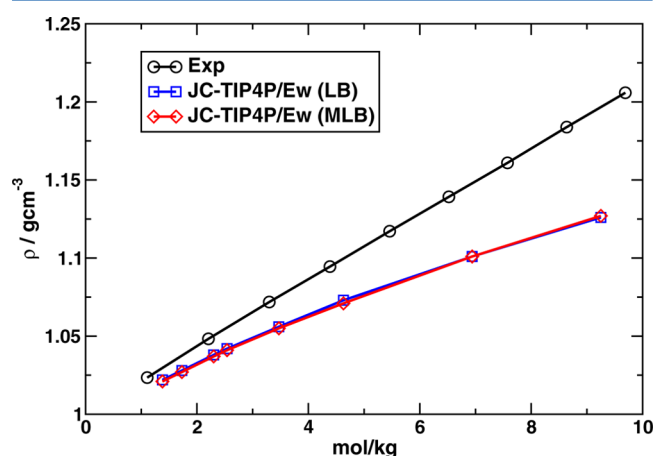
Table 6. Thermodynamic Results Using MLB Rules[a]

N_{ions}	%	mol/kg	U (kJ/mol^{-1})	V (nm^3)	ρ (g/cm^3)
24	2.4	1.38	−65.78	14.886	1.021
30	3.0	1.73	−70.32	15.005	1.027
40	4.0	2.30	−77.67	15.203	1.037
44	4.4	2.54	−80.53	15.282	1.041
60	5.9	3.47	−91.49	15.612	1.055
80	7.7	4.63	−104.31	16.031	1.071
120	11.0	6.94	−127.28	16.881	1.101
160	14.0	9.25	−147.24	17.733	1.127

[a]Internal energies are given in kJ mol^{-1} (per mol of particles $N_+ + N_-$ + N_{H_2O}). The number of water molecules is 480 for each solution.

deviations from the LB mixing rules. For an addition of almost 60% of salt, the volume increases an order of 20%, while the density increases only for an amount of about 10%. The packing fraction of the solution (ϕ) has also been tabulated in Table 5. The packing fraction increases almost linearly with the ion concentration, which reflects the capacity of water to host ions. Moreover, ϕ increases as long as ions and water molecules fill up approximately 75% of the total volume at the highest concentration. The small size of the Li^+ ions reduces the coordination number of water molecules around them (see Table 4), and then, the packing of Li^+ ions is less effective with

respect to the packing induced by bigger ones, such as Na^+.[69] However, it is also the small size of Li^+ ions that allows the system to accommodate a higher number of them. These results indicate the great capacity of water of incorporating ions. The configurational energy strongly decreases when the water–water HB interactions are replaced by the strong Coulombic water–ion interactions. The potential energy becomes considerably more negative at increasing ion concentration. The absolute value increases on the order of 120% from the lowest to the highest concentration. The fact that similar results are found with the use of LB and MLB rules indicates that the ion pairing does not play a relevant role in the macroscopic thermodynamic behavior.

In Figure 12, the densities of LiCl solutions predicted by the JC-TIP4P-Ew force field are compared with the experimental

Figure 13. Diffusion coefficient of Li^+ and Cl^- in solution as a function of concentration obtained with the use of LB and MLB rules. The same quantity for water is reported in the inset.


Figure 12. Density versus LiCl molality for the JC-TIP4P-Ew force field using LB rules (squares and blue line) and MLB (diamonds and red line) compared to the experimental values.[70]

results as a function of the concentration. The experiments show a linear increase for the whole range of concentration. In simulation, the density for low concentration has a linear increase with a value not so far from the experimental result, but with increasing concentration, there is a bending of the curve that deviates from the experimental trend.

It has also been already shown that the JC force field tailored for the SPC/E water model fails in reproducing the experimental density of NaCl solutions.[49] However, the JC-SPC/E provides a better description of the density of NaCl solutions, that is overestimated by about 2%, whereas the JC-TIP4P-Ew underestimates the density of the LiCl solutions by about 8%. Therefore, the JC ionic force field does not reproduce all salt solutions with the same accuracy. On the basis of this, the JC ionic force field should be corrected to increase the density of the LiCl solutions. One possibility would be to modify the LB rules, but in this case, the water–ion interactions, which is the only way to increase the density of the system without reparameterizing the force field.[17] The modification of the water–ion interactions has not been considered in this work; however, one should reduce the value of η in eq 2 to reduce the O-ion distance, and hence increase the density of the system.

In Figure 13, the diffusion coefficients of water and ions are reported as a function of concentration. The trend is a decrease of the diffusion at increasing concentration for both cases of LB and MLB rules. As reported in the inset of the figure, the
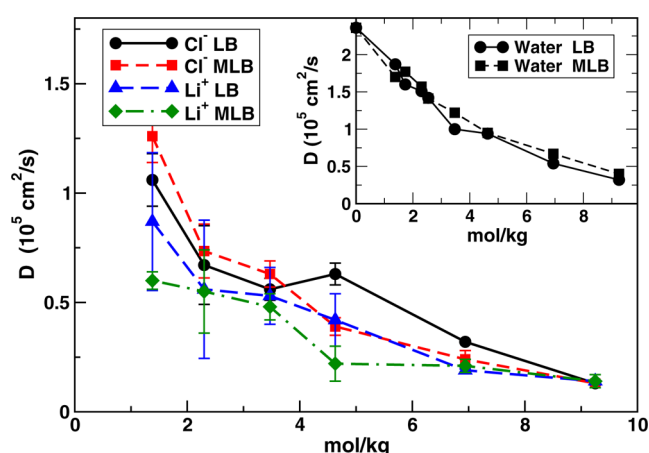
diffusion coefficient of the water molecules shows a similar behavior with the use of LB or MLB rules; however, the application of the MLB rules slightly increases the diffusivity at high concentration.

For Li^+ ion at the lowest concentration (2.4%), when the LB rules are applied, we get a value of 1.11×10^5 cm²/s, very close to the value 1.22×10^5 cm²/s obtained for Li^+ interacting only with water.[71] At this concentration, the cation–anion and cation–cation interactions are very weak, as can be deduced from the low peak of the $g_{LiCl}(r)$ in Figure 1. Switching on the MLB correction of the cation–anion potential the diffusion of Li^+ strongly decreases. It remains below the values obtained with the LB interaction at moderate concentrations. For the Li^+ ions, the diffusion seems little affected by the hydration. The cage of the water molecules around the cations is well-defined, and it does not change much with concentration or with the switching on of the corrections to LB rules (see Figure 9). Instead, the Cl^- ion diffusion appears to depend mainly on the hydration. The D of Cl^- decays with a trend similar to water for both LB and MLB calculations, MLB induces a faster decay at high concentration. By considering the first shell of $g_{ClO}(r)$ in Figure 10, it is clear that the MLB potential makes broader the cage around cations, enhancing the time of escaping. We note that the diffusion coefficients of the ions converge to similar values at high concentration; this also indicates the tendency of the ions to clusterize.

7. TRANSFERABILITY OF THE IONIC FORCE FIELD: JC-TIP4P/2005 FORCE FIELD

As it has been previously discussed, depending on the aims of the study, the choice of the ionic force field can be biased by the water potential model, since they are constructed around specific water models. The transferability of the JC-TIP4P-Ew ions to the TIP4P/2005 was recently tested by Moucka et al.[55] for NaCl aqueous solutions. They calculated the NaCl chemical potential in water and estimated its solubility in water TIP4P/2005. They obtained good agreement with the results with TIP4P-Ew, both for the variation of the electrolyte chemical potential with concentration and for the value of solubility.

Therefore, we tested the LiCl JC force field tailored with the TIP4P-Ew for its transferability to the TIP4P/2005 water model, a potential that has been successfully used to study water upon supercooling.

In Figures 14 and 15, we present the RDF obtained with the two different force fields for water. The comparison is done
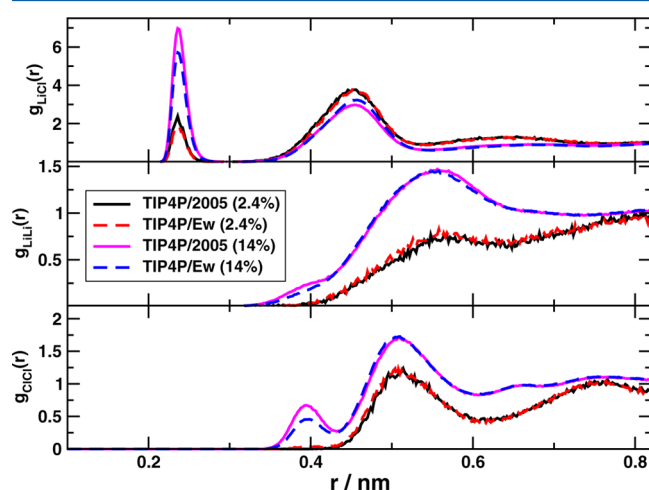
Figure 14. Li−Cl, Li−Li, and Cl−Cl RDFs using the JC-TIP4P-Ew parameter with the TIP4P/2005 (solid lines) and TIP4P-Ew (dashed lines) water potential models for two concentrations, 2.4 and 14%.

Figure 15. O−O, Li−O, and Cl−O RDFs using the JC-TIP4P-Ew parameter with the TIP4P/2005 (solid lines) and TIP4P-Ew (dashed lines) water potential models for two concentrations, 2.4 and 14%. For the Li−O and Cl−O RDFs, the 14% curves are shifted by 2.5 and 0.5 upward, respectively.
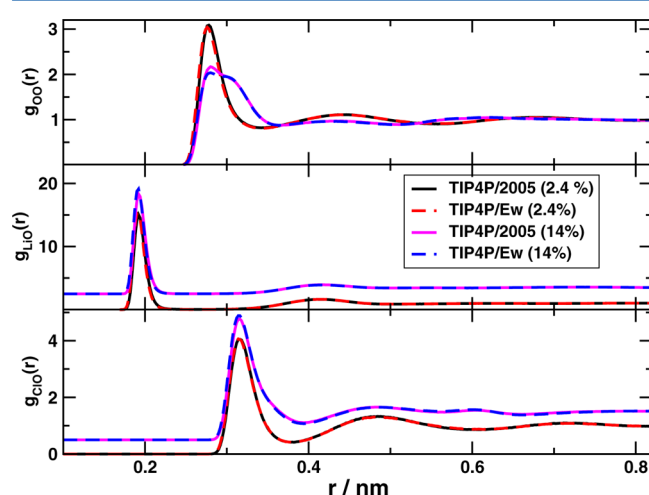
with the use of LB rules. The JC-TIP4P/2005 combination gives results very similar to the original JC-TIP4P-Ew.

Concerning the ion pairing, the $g_{LiCl}(r)$ is almost unchanged and the only difference between the results of the two force fields is a small enhancement of the prepeak in the $g_{ClCl}(r)$ at lower distances (0.39 nm) at high concentrations; see Figure 14.

The hydration shells of both ions are not modified by the water model change neither at low nor high concentrations (Figure 15). The small difference in the $g_{OO}(r)$ corresponds to the slight differences between the two water models in the absence of solutes. The increasing concentration induces the same changes on the RDF with a shoulder that appears on the left side of the main peak (Figure 15).

We have also compared the thermodynamic and kinetic properties predicted by JC-TIP4P-Ew and JC-TIP4P/2005. As

for the structural properties, both force fields produce essentially the same thermodynamic properties (see Tables 5 and 7). The main difference between them is on the internal

Table 7. JC-TIP4P/2005 Thermodynamic Results Using LB Rules[a]

N_{ions}	%	mol/kg	U (kJ/mol)	V (nm³)	ρ (g/cm³)
24	2.4	1.38	−67.81	14.839	1.024
160	14.0	9.25	−147.88	17.782	1.124

[a]Internal energies are given in kJ mol⁻¹ (per mol of particles N_{ions} + N_{H_2O}). The number of water molecules is 480 for each solution.

energy of the solution, and this difference is more evident at the lowest concentration; the macroscopic properties are dominated by the water−water interactions. However, the density difference remains constant for all salt concentrations. The diffusion coefficients obtained using the JC-TIP4P/2005 force field are also in good agreement with the original JC-TIP4P-Ew. The main difference is for the Li⁺, $0.141(20)10^{-5}$ cm² s⁻¹ for the JC-TIP4P-Ew and $0.096(20)10^{-5}$ cm² s⁻¹ for the JC-TIP4P/2005 for the most concentrated solution; in any case, both results are within the error bars.

Summarizing, the JC-TIP4P/2005 force field produces very similar results.

As we have previously discussed, the ion pairing structure can be corrected including deviations to the LB combining rules. By repeating the same procedure used before, we found that a proper set of MLB parameters for the JC-TIP4P/2005 potential is $\chi = 1.88$ and $\eta = 0.934$, very close to the MLB corrections for the JC-TIP4P-Ew. Thus, it can be concluded that also with the MLB rules there is a close agreement between the results obtained with the two different choices for the water model.

8. CONCLUSIONS

We performed computer simulations of aqueous solutions of LiCl under ambient conditions as a function of ionic concentration with the recent potential proposed by JC adapted for the TIP4P-Ew water model. The range of concentrations was varied from 2.4 to 14% mol of solute. The original JC potential, where the Lorentz−Berthelot (LB) rules are used, does not reproduce the experimental LiCl ion pairing. We checked that the agreement can be obtained by introducing a modification of the Lorentz−Berthelot (MLB) rules in the LiCl cross-interaction. With MLB rules, the behavior of the first peak height of the $g_{LiCl}(r)$ as a function of concentration is in agreement with the trend found in experiments. Concerning the $g_{LiLi}(r)$ and $g_{ClCl}(r)$ RDFs, the MLB potential predicts stronger effects for increasing concentration, in particular with an enhancement of a prepeak at shorter distances from the first shell at low concentration. This indicates that MLB rules favor a tendency to phase separation.

In analogy with other ionic aqueous solutions, the LiCl salt affects particularly the second shell of the $g_{OO}(r)$. While the hydrogen bond is preserved, the tetrahedral structure of the water network is modified by increasing concentration of ions, as has been observed for other salt solutions.[28,67,68] This behavior is similar to LB rules or including deviations. The MLB rules, however, show trends in better agreement with results on NaCl(aq)[67] and on KCl(aq).[67,72]

The hydration shells of Li⁺ show small changes with concentration. At increasing salt concentration, the intensity

of the first Li−O peak increases with LB and decreases with MLB rules. The use of MLB produces more marked changes as a function of concentration on the hydration shells of Cl^- with the appearance of a shoulder on the right side of the $g_{ClO}(r)$ peak.

The potential with MLB corrections makes the tendency of *clusterization* of ions more evident. This was predicted in large scale simulations of ions in water modeled with the mW potential[26] for increasing concentrations from 5% to the limiting value 20%, for which an incipient phase segregation was found upon cooling.

Ion pairing does not appear to play an important role in determining the macroscopic thermodynamic behavior of LiCl aqueous solutions, while the diffusion of ions shows a similar trend with concentration but differences due to the use of MLB are observed and they are more marked for Li^+ ions.

From the results of our computer simulations, there are indications that the JC potential in conjunction with the TIP4P-Ew reproduces well-known trends of ionic aqueous solutions found in experiments and computer simulations. The use of MLB rules improves the agreement with experiments for the ion−ion structural properties, while it has not much of an effect on the water structure apart from the highest concentrations investigated for which there are not experimental results to compare. Preliminary calculations at lower temperatures indicate that the simulation shows a similar trend to the experimental findings; for instance, the first peak of the Li−Cl RDF increases at low temperature and the second peak is almost unaffected. We plan future extended studies in the supercooled states.

The interesting features found in the ion diffusion deserve further work. We think that the improvement of the JC potential proposed in this work can be of great help in future studies, and we highlight the importance of including deviations of the LB rules to obtain a proper description of the structure of ion solutions in water. This type of approach has started to be considered in the literature,[20,32,49,52] since the necessity of incorporating deviations into the LB combining rules has become evident to properly describe the interaction between cations and anions.

By considering that the ionic force fields are constructed around specific water models, it is of great interest to test the transferability of the JC ion potential to other successful water models.[55] We have tested in LiCl(aq) the transferability of the JC ion potential to the TIP4P/2005 water model[56] for the purpose of future works under supercooled conditions. We have observed that both force fields, JC-TIP4P-Ew and JC-TIP4P/2005, produce the same results.

By taking into account the results obtained by Moucka et al.,[55] it can be deduced that the transferability of the JC-TIP4P-Ew ions to the JC-TIP4P/2005 force fields is valid for LiCl and NaCl. Given that these two water models are quite similar in many respects like geometry, fitted target properties, and application of the Berendsen polarization correction,[44] we would expect that this transferability would be verified more in general.

We expect that this work will stimulate experimental studies with the aim to elucidate the structure of aqueous solutions as a function of ionic concentration and in particular in the case of LiCl(aq) upon supercooling. New experimental results would allow the ionic force fields to be checked and improved. In addition, this study may be helpful to the study of other related structural effects such as the proposed ion chain formation in solution.[73−75] For future work, it will be interesting to analyze these effects. Despite the amount of work carried out so far, there is still room for further enhancements, especially in view of further studies of aqueous solutions approaching glassy phases.

■ ASSOCIATED CONTENT

Ⓢ Supporting Information

Figures showing snapshots of different configurations along the simulation trajectory using LB rules for the most diluted LiCl solution (2.4 %) and using MLB rules for the most diluted LiCl solution (2.4 %). This material is available free of charge via the Internet at http://pubs.acs.org.

■ AUTHOR INFORMATION

Corresponding Author
*E-mail: gallop@fis.uniroma3.it.

Notes
The authors declare no competing financial interest.

■ ACKNOWLEDGMENTS

■ REFERENCES

(1) Gurney, R. W. *Ionic Processes in Solutions*; McGraw Hill: New York, 1953.

(2) Hills, G. J.; Covington, A. K.; Lilley, T. H. In *Electrochemistry*; Hills, G. J., Ed.; The Chemical Society: London, 1970; Vol. *1*, Chapter Electrolyte Solutions, pp 1−55.

(3) Burgess, J. *Metals Ion in Solution*; John Wiley & Sons: Chichester and New York, 1979.

(4) Conde, M. R. Properties of Aqueous Solutions of Lithium and Calcium Chlorides: Formulations for Use in Air Conditioning Equipment Design. *Int. J. Therm. Sci.* **2004**, *43*, 367−382.

(5) Friend, J. A. N.; Colley, A. T. W. The Solubility of Lithium Chloride in Water. *J. Chem. Soc.* **1931**, *CCCCXXXIV*, 3148.

(6) Tromp, R. H.; Neilson, G. W.; Soper, A. K. Water Structure in Concentrated Lithium Chloride Solutions. *J. Chem. Phys.* **1992**, *96*, 8460−8469.

(7) Narten, A. H.; Vaslow, F.; Levy, H. A. Diffraction Pattern and Structure of Aqueous Lithium Chloride Solutions. *J. Chem. Phys.* **1973**, *58*, 5017−5023.

(8) Herdman, G. J.; Neilson, G. W. Neutron Scattering Studies of Aqua-Ions. *J. Mol. Liq.* **1990**, *46*, 165−179.

(9) Newsome, J. R.; Neilson, G. W.; Enderby, J. E. Lithium Ions in Aqueous Solution. *J. Phys. C: Solid State Phys.* **1980**, *13*, L923−L926.

(10) Copestake, A. P.; Neilson, G. W.; Enderby, J. E. The Structure of a Highly Concentrated Aqueous Solution of Lithium Chloride. *J. Phys. C: Solid State Phys.* **1985**, *18*, 4211−4216.

(11) Prevel, B.; Jal, J. F.; Dupuy-Philon, J.; Soper, A. Structural Characterization of an Electrolytic Aqueous Solution, LiCl - 6H2O, in the Glass, Supercooled Liquid, and Liquid States. *J. Chem. Phys.* **1995**, *103*, 1886−1896.

(12) Winkel, K.; Seidl, M.; Loerting, T.; Bove, L. E.; Imberti, S.; Molinero, V.; Bruni, F.; Mancinelli, R.; Ricci, M. A. Structural Study of Low Concentration LiCl Aqueous Solutions in the Liquid, Super-

cooled, and Hyperquenched Glassy States. *J. Chem. Phys.* **2011**, *134*, 024515.

(13) Harsanyi, I.; Bopp, P. A.; Vrhovšek; Pusztai, L. On the Hydration Structure of LiCl Aqueous Solutions: A Reverse Monte Carlo Based Combination of Diffraction Data and Molecular Dynamics Simulations. *J. Mol. Liq.* **2011**, *158*, 61–67.

(14) Harsanyi, I.; Pusztai, L. On the Structure of Aqueous LiCl Solutions. *J. Chem. Phys.* **2005**, *122*, 124512.

(15) Harsanyi, I.; Pusztai, L. Hydration Structure in Concentrated Aqueous Lithium Chloride Solutions: a Reverse Monte Carlo Based Combination of Molecular Dynamics Simulations and Diffraction Data. *J. Chem. Phys.* **2012**, *137*, 204503.

(16) Ibuki, K.; Bopp, P. A. Molecular Dynamics Simulations of Aqueous LiCl Solutions at Room Temperature through the Entire Concentration Range. *J. Mol. Liq.* **2009**, *147*, 56–63.

(17) Deublein, S.; Vrabec, J.; Hasse, H. A Set of Molecular Models for Alkali and Halide Ions in Aqueous Solution. *J. Chem. Phys.* **2012**, *136*, 084501.

(18) Degreve, L.; Mazze, F. M. Molecular Simulation of LiCl Aqueous Solutions. *Mol. Phys.* **2003**, *101*, 1443–1453.

(19) Pluharova, E.; Mason, P. E.; Jungwirth, P. Ion Pairing in Aqueous Lithium Salt Solutions with Monovalent and Divalent Counter-Anions. *J. Phys. Chem. A* **2013**, *117*, 11766–11773.

(20) Fyta, M.; Netz, R. R. Ionic Force Field Optimization Based on Single-Ion and Ion-Pair Solvation Properties: Going beyond Standard Mixing Rules. *J. Chem. Phys.* **2012**, *136*, 124103.

(21) Mishima, O. Application of Polymorphism in Water to Spontaneous Crystallization of Emulsified LiCl-H2O Solution. *J. Chem. Phys.* **2005**, *123*, 154506.

(22) Mishima, O. Phase Separation in Dilute LiCl-H2O Solution Related to the Polyamorphism of Liquid Water. *J. Chem. Phys.* **2007**, *126*, 244507.

(23) Suzuki, Y.; Mishima, O. Sudden Switchover between the Polyamorphic Phase Separation and the Glass-to-Liquid Transition in Glassy LiCl Aqueous Solutions. *J. Chem. Phys.* **2013**, *138*, 084507.

(24) Angell, C. A.; Sare, E. Liquid-Liquid Immiscibility in Common Aqueous Salt Solutions at Low Temperatures. *J. Chem. Phys.* **1968**, *49*, 4713–4714.

(25) Angell, C. A.; Sare, E. Glass-Forming Composition Regions and Glass Transition Temperatures for Aqueous Electrolyte Solutions. *J. Chem. Phys.* **1970**, *52*, 1058–1068.

(26) Le, L.; Molinero, V. Nanophase Segregation in Supercooled Aqueous Solutions and Their Glasses Driven by the Polyamorphism of Water. *J. Phys. Chem. A* **2011**, *115*, 5900–5907.

(27) Corradini, D.; Rovere, M.; Gallo, P. A Route to Explain Water Anomalies from Results on an Aqueous Solution of Salt. *J. Chem. Phys.* **2010**, *132*, 134508.

(28) Corradini, D.; Rovere, M.; Gallo, P. Structural Properties of High Density and Low Density Water in Supercooled Aqueous Solutions of Salt. *J. Phys. Chem. B* **2011**, *115*, 1461–1468.

(29) Corradini, D.; Gallo, P. Liquid-Liquid Critical Point in NaCl Aqueous Solutions: Concentration Effects. *J. Phys. Chem. B* **2011**, *115*, 14161–14166.

(30) Gallo, P.; Corradini, D.; Rovere, M. Excess Entropy of Water in a Supercooled Solution of Salt. *Mol. Phys.* **2011**, *109*, 2069–2079.

(31) Bankura, A.; Carnevale, V.; Klein, M. L. Hydration Structure of Salt Solutions from ab Initio Molecular Dynamics. *J. Chem. Phys.* **2013**, *138*, 014501.

(32) Cavallari, M.; Cavazzoni, C.; Ferrario, M. Structure of NaCl and KCl Concentrated Aqueous Solutions by ab Initio Molecular Dynamics. *Mol. Phys.* **2004**, *102*, 959–966.

(33) Krekeler, C.; Delle Site, L. Solvation of Positive Ions in Water: The Dominant Role of Water-Water Interaction. *J. Phys.: Condens. Matter* **2007**, *19*, 192101.

(34) Ghosh, M. K.; Re, S.; Feig, M.; Sugita, Y.; Choi, C. H. Interionic Hydration Structures of NaCl in Aqueous Solution: A Combined Study of Quantum Mechanical Cluster Calculations and QM/EFP-MD Simulations. *J. Phys. Chem. B* **2013**, *117*, 289–295.

(35) Luo, Y.; Jiang, W.; Yu, H.; MacKerell, A. D.; Roux, B. Simulation Study of Ion Pairing in Concentrated Aqueous Salt Solutions with a Polarizable Force Field. *Faraday Discuss.* **2013**, *160*, 135–149.

(36) Tainter, C. J.; Pieniazek, P. A.; Lin, Y.-S.; Skinner, J. L. Robust Three-Body Water Simulation Model. *J. Chem. Phys.* **2011**, *134*, 184501.

(37) Aaqvist, J. Ion-water interaction potentials derived from free energy perturbation simulations. *J. Phys. Chem.* **1990**, *94*, 8021–8024.

(38) Lin, Y. S.; Auer, B. M.; Skinner, J. L. Water Structure, Dynamics, and Vibrational Spectroscopy in Sodium Bromide Solutions. *J. Chem. Phys.* **2009**, *131*, 144511.

(39) Jensen, K. P.; Jorgensen, W. L. Halide, Ammonium, and Alkali Metal Ion Parameters for Modeling Aqueous Solutions. *J. Chem. Theory Comput.* **2006**, *2*, 1499–1509.

(40) Jorgensen, W. L.; Chandrasekhar, J.; Madura, J. D.; Impey, R. W.; Klein, M. L. Comparison of Simple Potential Functions for Simulating Liquid Water. *J. Chem. Phys.* **1983**, *79*, 926–935.

(41) Dang, L. X.; Smith, D. E. Molecular Dynamics Simulations of Aqueous Ionic Clusters Using Polarizable Water. *J. Chem. Phys.* **1993**, *99*, 6950–6956.

(42) Smith, D. E.; Dang, L. X. Computer Simulations of NaCl Association in Polarizable Water. *J. Chem. Phys.* **1994**, *100*, 3757–3766.

(43) Dang, L. X. The Nonadditive Intermolecular Potential for Water Revised. *J. Chem. Phys.* **1992**, *97*, 2659–2660.

(44) Berendsen, H. J. C.; Grigera, J. R.; Straatsma, T. P. The Missing Term in Effective Pair Potentials. *J. Phys. Chem.* **1987**, *91*, 6269–6271.

(45) Joung, I. S.; Cheatham, T. E., III. Determination of Alkali and Halide Monovalent Ion Parameters for Use in Explicitly Solvated Biomolecular Simulations. *J. Phys. Chem. B* **2008**, *112*, 9020–9041.

(46) Auffinger, P.; Cheatham, T. E., III; Vaiana, A. C. Spontaneous Formation of KCl Aggregates in Biomolecular Simulations: A Force Field Issue? *J. Chem. Theory Comput.* **2007**, *3*, 1851–1859.

(47) Horn, H. W.; Swope, W. C.; Pitera, J. W.; Madura, J. D.; Dick, T. J.; Hura, G. L.; Head-Gordon, T. Development of an Improved Four-Site Water Model for Biomolecular Simulations: TIP4P-Ew. *J. Chem. Phys.* **2004**, *120*, 9665–9678.

(48) Fyta, M.; Kalcher, I.; Dzubiella, J.; Vrbka, L.; Netz, R. R. Ionic Force Field Optimization Based on Single-Ion and Ion-Pair Solvation Properties. *J. Chem. Phys.* **2010**, *132*, 024911.

(49) Aragones, J. L.; Sanz, E.; Vega, C. Solubility of NaCl in Water by Molecular Simulation Revisited. *J. Chem. Phys.* **2012**, *136*, 244508.

(50) Nerenberg, P. S.; Jo, B.; So, C.; Tripathy, A.; Head-Gordon, T. Optimizing Solute–Water Van der Waals Interactions to Reproduce Solvation Free Energies. *J. Phys. Chem. B* **2012**, *116*, 4524–4534.

(51) Mao, A. H.; Pappu, R. V. Crystal Lattice Properties Fully Determine Short-Range Interaction Parameters for Alkali and Halide Ions. *J. Chem. Phys.* **2012**, *137*, 064104.

(52) Aragones, J. L.; Sanz, E.; Valeriani, C.; Vega, C. Calculation of the Melting Point of Alkali Halides by Means of Computer Simulations. *J. Chem. Phys.* **2012**, *137*, 104507.

(53) Vega, C.; Abascal, J. L. F.; Conde, M. M.; Aragones, J. L. What Ice Can Teach Us About Water Interactions: a Critical Comparison of the Performance of Different Water Models. *Faraday Discuss.* **2009**, *141*, 251–276.

(54) Vega, C.; Abascal, J. L. F. Simulating Water with Rigid Non-Polarizable Models: a General Perspective. *Phys. Chem. Chem. Phys.* **2011**, *13*, 19663–19688.

(55) Moučka, F.; Lisal, M.; Smith, W. R. Molecular Simulation of Aqueous Electrolyte Solubility. 3. Alkali-Halide Salts and Their Mixtures in Water and in Hydrochloric Acid. *J. Phys. Chem. B* **2012**, *116*, 5468–5478.

(56) L.Abascal, J. F.; Vega, C. A General Purpose Model for the Condensed Phases of Water: TIP4P/2005. *J. Chem. Phys.* **2005**, *123*, 234505.

(57) Abascal, J. L. F.; Vega, C. Note: Equation of State and Compressibility of Supercooled Water: Simulations and Experiment. *J. Chem. Phys.* **2011**, *134*, 186101.

(58) Jorgensen, L.; Chandrasekhar, J.; Madura, J. D.; Impey, R. W.; Klein, M. L. Comparison of Simple Potential Functions for Simulating Liquid Water. *J. Chem. Phys.* **1983**, *79*, 926−935.

(59) der Spoel, D. V.; Lindahl, E.; Hess, B.; Groenhof, G.; Mark, A. E.; Berendsen, H. J. C. GROMACS: Fast, Flexible, and Free. *J. Comput. Chem.* **2005**, *26*, 1701−1718.

(60) Bussi, G.; Donadio, D.; Parrinello, M. Canonical Sampling through Velocity Rescaling. *J. Chem. Phys.* **2007**, *126*, 014101.

(61) Parrinello, M.; Rahman, A. Polymorphic Transitions in Single Crystals: a New Molecular Dynamics Method. *J. Appl. Phys.* **1981**, *52*, 7182−7190.

(62) Essmann, U.; Perera, L.; Berkowitz, M. L.; Darden, T.; Lee, H.; Pedersen, L. G. A Smooth Particle Mesh Ewald Method. *J. Chem. Phys.* **1995**, *103*, 8577−8593.

(63) Miyamoto, S.; Kollman, P. Settle: An Analytical Version of the SHAKE and RATTLE Algorithm for Rigid Water Models. *J. Comput. Chem.* **1992**, *13*, 952−962.

(64) NIST Center for Neutron Research Neutron scattering lengths and cross sections. http://www.ncnr.nist.gov/resources/n-lengths/, Accessed: Jan 3, 2014.

(65) Soper, A. K. Structural Transformations in Amorphous Ice and Supercooled Water and Their Relevance to the Phase Diagram of Water. *Mol. Phys.* **2008**, *106*, 2053−2076.

(66) Gubskaya, A.; Kusalik, P. The Total Molecular Dipole Moment for Liquid Water. *J. Chem. Phys.* **2002**, *117*, 5290−5302.

(67) Gallo, P.; Corradini, D.; Rovere, M. Ion Hydration and Structural Properties of Water in Aqueous Solutions at Normal and Supercooled Conditions: a Test of the Structure Making and Breaking Concept. *Phys. Chem. Chem. Phys.* **2011**, *13*, 19814−19822.

(68) Corradini, D.; Gallo, P.; Rovere, M. Molecular Dynamics Studies on the Thermodynamics of Supercooled Sodium Chloride Aqueous Solution at Different Concentrations. *J. Phys.: Condens. Matter* **2010**, *22*, 284104.

(69) Docherty, H.; Galindo, A.; Sanz, E.; Vega, C. Investigation of the Salting Out of Methane from Aqueous Electrolyte Solutions Using Computer Simulations. *J. Phys. Chem. B* **2007**, *111*, 8993−9000.

(70) Vercher, E.; Solsona, S.; Vazquez, M.; Martinez-Andreu, A. Apparent Molar Volumes of Lithium Chloride in 1-Propanol+ Water in the Temperature Range from 288.15 to 318.15 K. *Fluid Phase Equilib.* **2003**, *209*, 95−111.

(71) Koneshan, S.; Rasaiah, J. C.; Lynden-Bell, R. M.; Lee, S. H. Solvent Structure, Dynamics, and Ion Mobility in Aqueous Solutions at 25° C. *J. Phys. Chem. B* **1998**, *102*, 4193−4204.

(72) Gallo, P.; Corradini, D.; Rovere, M. Do Ions Affect the Structure of Water? The Case of Potassium Halides. *J. Mol. Liq.* **2014**, *189*, 52−56.

(73) Thomas, A. S.; Elcock, A. H. Molecular Dynamics Simulations of Hydrophobic Associations in Aqueous Salt Solutions Indicate a Connection between Water Hydrogen Bonding and the Hofmeister Effect. *J. Am. Chem. Soc.* **2007**, *129*, 14887−14898.

(74) Fennell, C. J.; Bizjak, A.; Vlachy, V.; Dill, K. A.; Sarupria, S.; Rajamani, S.; Garde, S. Ion Pairing in Molecular Simulations of Aqueous Alkali Halide Solutions. *J. Phys. Chem. B* **2009**, *113*, 14837−14838.

(75) Fennell, C. J.; Bizjak, A.; Vlachy, v.; Dill, K. A. Ion Pairing in Molecular Simulations of Aqueous Alkali Halide Solutions. *J. Phys. Chem. B* **2009**, *113*, 6782−6791.